

Optimized Hybrid Rotation Invariant LBP fused Lightweight MobileNetV2 Model for Deep Visual Inspection of Apple Bruises

Pritha Chakraborty⁰⁰⁰⁹⁻⁰⁰⁰⁰⁻⁷⁷⁷⁸⁻⁷⁹⁷⁰^{1*}, Gunjan Mukherjee⁰⁰⁰⁰⁻⁰⁰⁰²⁻³⁹⁵⁹⁻³⁷¹⁸² and Jayanta Aich ⁰⁰⁰⁰⁻⁰⁰⁰³⁻³¹⁸⁷⁻⁰⁹³³^{3†}

^{1*}Computational Sciences, Brainware, 398, Ramkrishnapur Road, Barasat, Kolkata, 700125, WestBengal, India.

²Computational Sciences, Brainware, 398, Ramkrishnapur Road, Barasat, Kolkata, 700125, WestBengal, India.

³Computational Sciences, Brainware, 398, Ramkrishnapur Road, Barasat, Kolkata, 700125, WestBengal, India.

Abstract

Bruise detection in apples is a critical task which is faced in post-harvest quality control of the fruit. The bruises significantly impact consumer preference, shelf life, and overall market value of the fruit. Traditional inspection methods are labor-intensive, subjective and prone to inconsistencies. In order to cope up with huge number of production demands, the real necessity is felt in the development of efficient, automated, and non-destructive techniques. In this study, we have proposed an optimized rotational invariant local binary pattern (LBP) model fused with the light weight MobileNetV2. LBP offers local texture feature of the fruit. The rotation invariant feature of LBP avoids the rotational effects, likely to occur at the time of image capturing of the samples. The performance of hybrid model has been assessed by several metrics. The result of assessment was estimated at 98% for classification accuracy and a 0.98 for AUC measure of ROC curve, the model's initial findings demonstrate its efficiency.

Keywords: keyword1, Keyword2, Keyword3, Keyword4

1 Introduction

Apple is the most familiar and horticultural product consumed globally. Apple production covers 10% of the entire food yield chain of the world. China came first followed by Turkey standing at the third position in production line. The apple bruise occurs during picking, transportation and post harvest storage. The bruise produces local rotting and perishes the fruit causing severe economic loss in the bulk transportation specially in supply chain management. The rotting may be of higher degree depending on intensity or thrust. The early bruise detection of fruit within a few hours of the fall is the real challenge as sometimes the skin scar can not be visibly traced in naked eye. The conventional machine learning method also fails to properly detect the bruise with same precision and accuracy. Moreover the precision in local feature capturing can be performed poorly. However, the apple rot presents a significant challenge to the agricultural industry and supply chain, resulting in considerable financial losses and resource waste. If left unchecked, the deterioration of apple quality due to rot can severely impact marketability and lead to large-scale post-harvest losses, food quality control and minimizing wastage. To address this challenge, computer vision approach is adopted. The texture descriptor Local Binary Pattern (LBP) is used to extract the local texture feature depending on the individual pixels relative to neighboring pixels. The method has been annexed with the rotation invariance feature addressing the rotational variance during capturing. This also overcomes the illumination variation. The lightweight MobileNET V2 has been used for saving power and memory in handling the complex and large datasets. In this study, we propose an approach that combines rotation invariant Local Binary Pattern (LBP)

feature extraction with light weight MobileNetV2 for the automated detection of apple bruise in hand held device . This hybrid method uses the texturediscriminative power of LBP and the deep learning capabilities of CNNs to enhance detection performance. The developed model was evaluated using standard metrics such as accuracy, precision, recall, F1-score, and Receiver Operating Characteristic (ROC) curve analysis. The contributions of the current work can be summarized as

1. The improved hybrid framework for higher precision.
2. Optimized model fusion
3. Use of indigenous dataset.
4. Introduction of rotation invariance to the process.
5. The appointment of metrics for justified qualitative results evaluation supported by the quantitative support.

2 Related Work

Number of studies based on artificial intelligence in fruit sorting and quality assessment has been carried out [7] investigated the precision agriculture with use of AI. It revealed AI based enhancement of plant disease detection and automation and quality control in fruit sorting. It lacked on bruise detection in fruits. Koc, (2021) focused on image processing for fruit classification using machine vision technique based on external features. It offered insights into improving sorting efficiency. The work failed in producing proof of concept for early sign of the scars or bruise on the fruits. Paolo Valdez et al. (2021) showcased deep learning approach towards defect detection in apples with high accuracy. The early appearance of light skin scars on the fruits was not traced in the concerned work. Hwa et al. (2024) reviewed AI and robotics in the food industry. The bruise information was not much highlighted in this work. Wan (2020) applied Faster R-CNN for multi-class fruit detection. It effectively differentiated between fresh and rotten apples on the basis of texture , shape and color. The bruise could not be traced in this research. Pathmanaban et al. (2023) explored AI-based thermal imaging for post-harvest handling reducing the human interference . The detection of bruise in the early phases was absent in the concerned work. Li (2012) examined hyperspectral imaging for non-destructive quality assessment with AI enhanced imaging. The work could not respond much successfully to the bruise detection. Ahmed et al. (2023) highlighted AI's integration into smart agriculture, optimizing sorting, grading, and supply chain management. Lastly, Lopez et al. (2019) discussed limitations of AI-based food quality control. In spite of its advantages, challenges like variability in fruit quality still prevent the realworld deployment, pointing to areas needing further refinement. Tian et al. (2023) combined near-infrared (NIR) camera imaging with an adaptive threshold segmentation algorithm to detect bruises in the fruits within 30 minutes of impact. The accuracy of 95.6% with an F1-score of 94.7% outperformed traditional Otsu or fixedthreshold approaches but the method was very costly and comparatively complex. Gai et al. (2022) introduced a Spectral-CNN, achieving 95.8% accuracy using 20 characteristic wavelengths. The method failed to provide the cost effective solution. Yang et al. (2024) proposed an improved MobileViT (iM-ViT) network to process hyperspectral images across 397–1004nm. The procedure was relatively costlier. A 2025 study used a self-designed multispectral imaging system along with an improved advanced decoder with F1 scores up to 97.5%, while a DenseNet-based model classified bruise severity and timing with 99% accuracy.

3 Method

3.1 Data Collection

The set of data for analysis comprises 1,000 images for apples are taken with high resolution camera (Sony) . The apples species have been purchased from the local fruit market of Kolkata and the images of fruits have been captured in natural light condition preserving the texture, shape, and color from the environmental hazards. [12,14]. The dataset includes images taken from different orientations, such as front, side, and angled views[15] [6,13]. Dataset of the apples are shown in Fig 1 which clearly shows a (a)fresh apple but (b) shows a small area of the apple which is not visible in naked eye . This portion leads to rotting of the apple started gradually from that small bruised portion. The dataset has been further augmented for achieving more higher accuracy.



Fig. 1: (a) first picture; (b) second picture.

3.2 Pre-processing

The images of apples were collected in broad day light and also in night so elimination of noises contained in it requires some elimination process. The collected images were subjected to the preprocessing techniques followed by feature extraction and successive classification [2,16]. The procedure includes the resizing of pixels to a uniform dimension of 256 x 256 pixels to ensure consistency all along the dataset, for suitability of deep learning models. Next, pixel values were normalized with in the range between 0 and 1, for standardizing intensity values and improving the efficiency and stability of model training process [16].The images were denoised and background subtracted in order to achieve higher accuracy and precision [17].

3.3 Feature Extraction using LBP

The Local Binary Pattern (LBP) approach was used for feature extraction for identifying the subtle textural differences [4]. Instead of using global feature extraction techniques, LBP highlights minute surface changes. The deterioration was found by encoding local intensity variations [4,9]. The resilience of process against the abrupt change of illumination with rotational invariance efficiently provide computing results[10,14]. The underlying principle includes surrounding connectivity of each of the pixels with neighboring ones. [9,13,14]. The LBP operator assigns a binary value to each pixel, forming a unique pattern that encodes texture variations [8,13,15].

2. Basic LBP Operator

The basic LBP operator works with a 3 x 3 neighborhood of a pixel. The central pixel value is used as a threshold to generate an 8-bit binary code. Given a central pixel I_c and its 8 neighboring pixels I_n , the LBP code is computed as

$$P-1$$

$$LBP = \sum_{n=0}^{P-1} s(I_n - I_c) 2^n \quad (1)$$

Where I_c is intensity of central pixel. I_n is the intensity of the n-th neighbor. P is the number of neighbors (usually 8). $s(x)$ is a step function defined as:

3. Circular LBP and Rotation Invariance

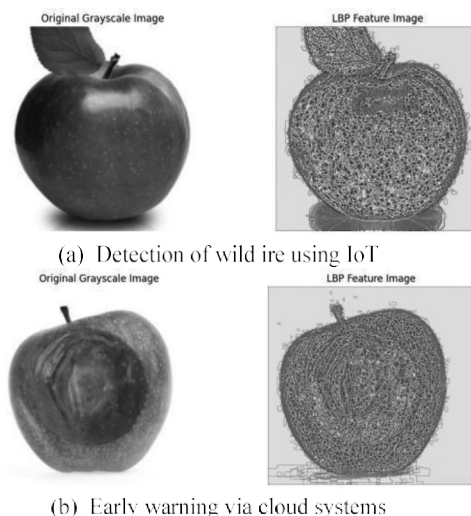
To handle scaling and rotation, a circular neighborhood of radius R is used:

$$P-1$$

$$LBP_{P,R} = \sum_{p=0}^{P-1} s(I_p - I_c) 2^p \quad (2)$$

Where I_p is the gray value of the p-th sampling point on a circle of radius R around the center pixel. The rotation invariant LBP feature extraction involves the local features of the fruit. The extracted image features and the corresponding feature vectors for the fresh and bruised apples are shown in the Fig.??

In Fig. ?? ref the image of the fresh apple and its corresponding LBP features are shown. Similarly, the bruised apples and corresponding LBP feature images are presented in Fig ???. The prominence of local features are obvious in both of the images. AI Model Architecture



The proposed model utilizes MobileNetV2, a lightweight and computationally efficient variant of the VNet architecture, adapted to process 2D apple images for bruise classification. MobileNetV2 model inherits the U-Net/V-Net encoder-decoder structure, while integrating the depthwise separable convolutions and inverted residual blocks from MobileNet to reduce parameter count and computational complexity. The encoder consists of multiple down sampling stages, where each stage applies depthwise separable convolutions followed by point wise convolutions and ReLU6 activations. These are wrapped within inverted residual blocks to preserve feature representation while minimizing information loss. The decoder path mirrors the encoder structure, employing up sampling layers followed by convolutional layers to reconstruct spatial features and localize bruising patterns. A skip connection mechanism is used between corresponding encoder and decoder blocks to retain spatial context, which is particularly important for detecting small, localized bruises. The final layer of MobileNetV2 outputs a dense feature representation, which is subsequently fused with LBP features before being passed to the classifier. This architecture achieves an optimal trade-off between accuracy and efficiency, making it well-suited for deployment on mobile and edge devices used in real-time fruit inspection systems.

2. MobileNet Block: Depthwise Separable Convolutions

MobileNet comprises depthwise separable convolutions instead of standard convolutions which aids in reduction of cost.

2.1 Standard Convolution

A standard convolutional layer with input feature maps of size $H \times W \times M$ and output channels N , using kernel size $K \times K$, requires. The cost function is presented in

$$Cost_{standard} = K^2 \cdot M \cdot N \cdot H \cdot W \quad (3)$$

Depthwise convolution layer consists of one $K \times K$ filter per input channel. The

$$Cost_{depthwise} = K^2 \cdot M \cdot H \cdot W \quad (4)$$

Point wise convolution (1×1) combines M channels into N channels. The cost function is estimated in Eq.5 and the total cost for the model is expressed in Eq.6

$$\text{Cost}_{\text{pointwise}} = M \cdot N \cdot H \cdot W \tag{5}$$

Total cost for the model taking into consideration the constituent layers,

$$\text{Cost}_{\text{MobileNet}} = K^2 \cdot M \cdot H \cdot W + M \cdot N \cdot H \cdot W \tag{6}$$

This is much less than standard convolution when $K = 3$ and M, N are large. The model architecture is shown in the Fig.3 . The LBP features of the apple fruit images are fed into MobileNetV2 model. The layer wise percolation of image features and its inal classification is shown also in the Fig.3

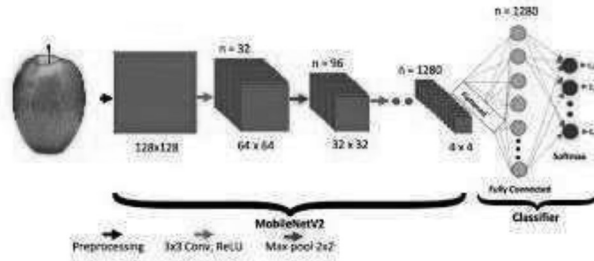


Fig. 3: (a) first picture; (b) second picture.

The algorithm on optimized rotation invariant LBP fusion with light weight MobileNetV2 model is presented in following subsection.

3.4 Algorithm: Optimized Rotation-Invariant LBP Fused with MobileNetV2 Complexity Estimation

First the optimized rotation-invariant Local Binary Pattern (LBP) is computed for each pixel in the input image of size $M \times N$. Each pixel is surrounded by the P number of different pixels. The time complexity per pixel is $O(P^2)$ and total complexity of $O(MNP^2)$ for the entire image. Since P is typically a small constant (e.g., 8), this stage remains computationally feasible. For the MobileNetV2 model , the complexity of the model operation can be expressed as $O(D)$, where D accounts for the fixed computational cost of MobileNetV2’s convolutional layers and global average pooling. The L2 normalization and concatenation of the LBP and MobileNetV2 feature vectors, $f_{\text{LBP}} \in R^{d_1}$ and $f_{\text{MNet}} \in R^{d_2}$ respectively. Where d_1 and d_2 implies respective dimensions of feature vectors. These operations are linear in the size of the vectors, giving a complexity of $O(d_1 + d_2)$. So the total complexity of the combined model can be stated as

$$T(n) = O(MNP^2 + D + d_1 + d_2) \tag{7}$$

The space complexity consists of the size of matrix representing the image under consideration and dimensions of the feature spaces.

$$S(n) = O(MN + d_1 + d_2) \tag{8}$$

3.5 Model Training

The proposed LBP-Mobile-VNet model was trained using the Adam optimizer, known for its efficient convergence and adaptive learning capabilities [5–7]. A learning rate of 0.001 was chosen, which is

ϵ
 $M \times N \times 3$

Algorithm 1 Optimized Rotation-Invariant LBP with MobileNetV2 Feature Fusion
 1: Input: Image I R
 2: Output:

Fused Feature Vector F

- 3: function OptimizedLBP MobileNetFusion(I)
- 4: Resize I to 224×224 for MobileNetV2 compatibility
- 5: // Step 1: Compute Optimized Rotation-Invariant LBP
- 6: for each pixel p with center (x,y) do
- 7: Sample P neighbors on a circle of radius R:

$$g_p = \{g_0, g_1, \dots, g_{P-1}\}$$

- 8: Compute LBP pattern:

$$LBP_{P,R}(x,y) = \sum_{p=0}^{P-1} s(g_p - g_c) \cdot 2^p$$

where

$$s(x) = \begin{cases} 1 & x \geq 0 \\ 0 & x < 0 \end{cases}$$

- 9: Compute all circular bitwise rotations of $LBP_{P,R}$
- 10: Select minimum rotation-invariant code:

$$LBP_{ri}(x,y) = \min\{ROR(LBP_{P,R},i) \mid 0 \leq i < P\}$$

- 11: end for

$\in d_1$

- 12: Flatten the resulting LBP_{ri} image into vector $f_{LBP} \in \mathbb{R}^{d_1}$
- 13: // Step 2: Extract Deep Features from MobileNetV2
- 14: Feed image I to pretrained MobileNetV2 (excluding classifier)

$\in d_2$ 15:

Extract global average pooling vector: $f_{MNet} \in \mathbb{R}^{d_2}$

- 16: // Step 3: Normalize and Fuse Features

$$\hat{f}_{LBP} = \frac{f_{LBP}}{\|f_{LBP}\|_2}, \quad \hat{f}_{MNet} = \frac{f_{MNet}}{\|f_{MNet}\|_2}$$

- 17: Concatenate features:

$$F = \hat{f}_{LBP} \parallel \hat{f}_{MNet} \in \mathbb{R}^{d_1+d_2}$$

- 18: return F
- 19: end function

widely regarded as optimal for most deep learning tasks. As the task involved binary classification distinguishing between fresh and bruised/rotting apples the categorical cross-entropy loss function was employed to minimize the error in prediction [5,11,22]. To enhance generalization and prevent over fitting, K-fold cross-validation was implemented. This strategy enabled a more reliable assessment

of the Mobile-VNet model’s performance on unseen data, especially given the subtle nature of early bruises [14–15]

3.6 Evaluation and Validation

The performance of the LBP-Mobile-VNet model was assessed using multiple evaluation metrics and visualization techniques. Receiver Operating Characteristic (ROC) curve, confusion matrix, and accuracy/loss curves [9] were used to validate the training behavior and classification performance. The images of fresh and bruised apples in different layers of the MobileNetV2 model are presented in the Fig .4

The layer wise view of extracted image of the fresh apple are shown in the Figure. The differences in layer wise extracted features for fresh and bruised apples are observable . The local feature extraction at the granular level has been performed layer wise for the MobileNetV2.

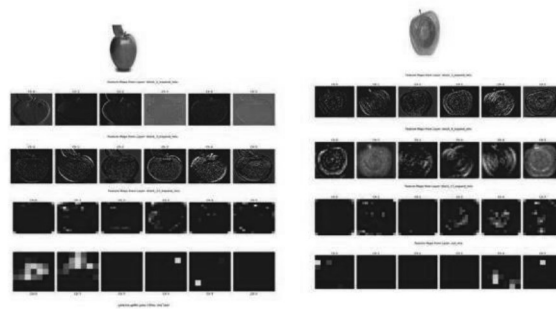


Fig. 4: (a) first picture; (b) second picture.

4 Results

The rotation invariant LBP integrated MobileNetV classifier model is used to carryout the classification on the local features of the fruit.The textural exchange and bruise has been detected efficiently by the model. The model has been trained with the Adam optimizer and validated via K-fold cross-validation.

The system shows strong classification accuracy, low loss, and stable convergence. This confirms the model’s suitability for deployment in real-world applications such as automated sorting and quality monitoring in agricultural and retail systems [3–7]. The histogram feature vectors are the features extracted from the image through LBP feature extraction process. The respective histogram features of the fresh and bruised apples are shown in the Table .1

Table 1: Extracted LBP histogram feature vector

Sample type	Mean (t)	Median (t)	Mode (t)	Standard Deviation (t)
Fresh non-bruised apple fruit	0.09999999999999999	0.05416	0.00984034	0.10629905078616887
Bruised apple fruit	0.099999998	0.04060465	0.00712661	0.1333554389827923

The differences between the estimated values for respective statistical functions are manifested from the Table. The differences if values between median, mode and standard deviation are considerable. The accuracy curve demonstrates a steady increase in model performance across 100 epochs, with training accuracy at 97% and validation accuracy at 98%. The proximity of these values to each other demonstrates that the model learns well from training samples and retains excellent generalization to new samples. The smooth convergence of the curve also verifies the reliability of the model, with no evidence of over fitting or loss of performance. These findings prove that the suggested CNN-LBP model, optimized with the Adam optimizer is appropriate for practical applications like automated sorting of apples in agriculture and retail sectors[23-24]. The accuracy and loss curve is shown in Fig5

The smooth convergence of the curve implies achievement and stability of the result. The corresponding loss computed also offers the good correlation with the accuracy.

The suggested CNN-LBP model optimized using the Adam optimizer's learning efficiency is further confirmed by the loss curves [3–4, 6–8]. As the model gains the ability to identify significant features in the input data, the training loss gradually decreases from its initial value of around 0.85. Likewise, the validation loss has a similar trajectory that closely resembles the training loss, suggesting little over fitting and efficient generalization. Both losses get close to zero by the 100th epoch, indicating that the model has performed at its best without over fitting or under training. This

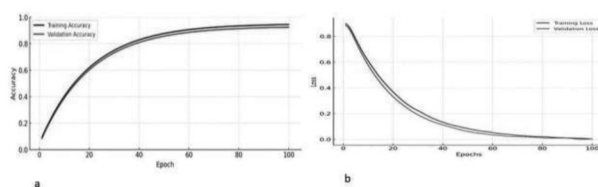


Fig. 5: (a) first picture; (b) second picture.

consistent drop in loss indicates that the CNN-LBP model using the Adam optimizer is effectively converging and optimizing for the classification of fresh and rotten apples. The model's resilience in correctly differentiating between rotten and fresh apples is further demonstrated by the smoothness of loss curves. The loss curves are displayed in Fig .5.

The confusion matrix presents a complete analysis of the performance of the CNN-LBP model[47] in distinguishing between fresh and rotten apples from a dataset of 1,000 images (500 fresh and 500 rotten). The matrix shows that 272 fresh apples were accurately labeled as fresh (True Positives) and 261 fresh apples were incorrectly labeled as rotten (False Negatives). Correspondingly, 244 spoiled apples were correctly labeled as spoiled (True Negatives), while 223 spoiled apples were wrongly assigned to the class fresh (False Positives).[24]. Such results tell us that the model performs rather symmetrically but faces some misclassifications, notably in discriminating some of the spoiled apples from the fresh apples. Matrix are demonstrate in fig. 6

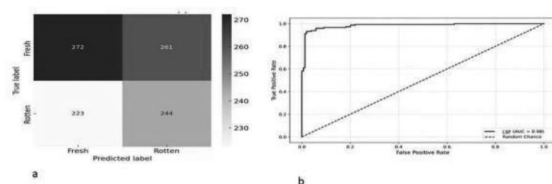


Fig. 6: (a) first picture; (b) second picture.

The Receiver Operating Characteristic (ROC) curve provides the model performance with respect to all the thresholds[5,23]. The ROC curve shows how well the model distinguishes between two classes at different thresholds by plotting True Positive Rate (TPR) against the False Positive Rate (FPR). With a high Area Under the Curve (AUC) value of 0.98, the model shows considerable capacity for categorization. The steep climb of the curve toward the upper-left corner indicates a high sensitivity with few false positives[9,16]. Furthermore, overall classification accuracy value of 95% demonstrates its dependability and efficiency in automated fruit quality evaluation, making it a useful instrument for practical agricultural applications. This confirms the efficacy of the classifying model based on LBP features of the fruit on CNN classifier [3-7]. The presented model works on the LBP features of apple. The performance characteristics of the suggested CNN-LBP model with the Adam optimizer for classifying fresh and rotten apples are shown in Table 3. With a 95% accuracy rate, the model proved to be successful in differentiating between rotting and fresh apples. While the recall (95.5%) shows that the model can accurately identify all fresh and rotten apples, the precision (94.8%) shows that a significant percentage of properly recognized fresh and rotten apples among the anticipated occurrences. The model’s balanced performance is further supported by the F1-score (95.15%), which is the harmonic mean of accuracy and recall. These findings demonstrate how deep learning may be used to automate the evaluation of apple quality, lower human error, and boost food supply chain efficiency. This explanation makes the importance of your model’s performance very evident.

The result obtained through the rotation invariant LBP fused MobileNETV2 model has been compared with some existing traditional models. The comparative study of the result obtained through respective metrics have been presented in the Table3.

Table 2: Performance comparison with conventional models

Classifier	Performance accuracy (%)
SVM	96%
CNN	97%
MobileNetV2	98%
LBP with MobileNetV2	98.5%

Table 3: Performance comparison with conventional models

Classifier	Performance accuracy (%)
SVM	96%
CNN	97%

MobileNetV2	98%
LBP with MobileNetV2	98.5%

The comparative study of different machine learning algorithm provides a critical glimpse of present research. Since the challenge lies in interpretation of textural defect of apple fruit invisible to the naked eye, the deep feature extraction can only reveal the condition of bruise and its aftermath impact in the post harvest stage. The accuracy measure of apple fruit with optimized hybrid model is 98.5% which far exceeds the accuracy values obtained in some other machine learning models. This vouches for the potential of the model towards the classification and detection of bruise with high precision.

5 Conclusion

In the agricultural and food supply chain, identifying rotten and fresh apples is a crucial part of quality control. Large-scale applications cannot benefit from the time-consuming, ineffective, and human errorprone nature of traditional manual inspection techniques. This paper suggested an AI-driven method to overcome these obstacles by combining Convolutional Neural Networks (CNN) with the Adam optimizer for effective training and convergence, and Local Binary Pattern (LBP) for feature extraction. The findings of the experiment show that the suggested model is a good option for automated fruit sorting and quality evaluation as it detects apple rotting with high accuracy. The efficacy of the model is confirmed by performance evaluation utilizing important measures including accuracy, precision, recall, F1-score, and the ROC curve.

The high identification accuracy 98% indicates that post-harvest losses can be decreased and efficiency can be greatly increased by incorporating deep learning techniques into agricultural operations. The results of this study aid in the creation of intelligent sorting systems that can enhance supply chain management, lower waste, and increase food quality. To improve classification accuracy even further and facilitate real-world deployment, future research can investigate combining multispectral photography with IoT-enabled realtime monitoring. This study emphasizes the value of implementing cutting-edge machine learning algorithms for automated quality control in fruit sorting and the possibility of AI-driven solutions in contemporary agriculture. In addition, the classifier model can also be implemented in the handheld device like mobile phone for ensuring the real time assessment of the fruit.

Acknowledgements are not compulsory. Where included they should be brief. Grant or contribution numbers may be acknowledged.

Please refer to Journal-level guidance for any specific requirements.

References

- [1] Edan, Y., Han, S., and Kondo, N. (2009). "Automation in agriculture." Springer Handbook of Automation, pp. 1095–1128.
- [2] Kamilaris, A., and Prenafeta-Boldu', F. X. (2018). "Deep learning in agriculture: A survey." *Computers and Electronics in Agriculture* 147, 70–90.
- [3] Kumar, A., Joshi, R. C., Dutta, M. K., Jonak, M., and Burget, R. (2021, October). "Fruit-CNN: An efficient deep learning-based fruit classification and quality assessment for precision agriculture." In *2021 13th International Congress on Ultra Modern Telecommunications and Control Systems and Workshops (ICUMT)*, pp. 60–65. IEEE.
- [4] Juefei-Xu, F., Boddeti, V. N., and Savvides, M. (2017). "Local binary convolutional neural networks." In *Proceedings of the IEEE Conference on Computer Vision and Pattern Recognition*, pp. 19–28.

- [5] Zhang, Z. (2018, June). "Improved Adam optimizer for deep neural networks." In 2018 IEEE/ACM 26th International Symposium on Quality of Service (IWQoS), pp. 1–2. IEEE.
- [6] Minaee, S., Kalchbrenner, N., Cambria, E., Nikzad, N., Chenaghlu, M., and Gao, J. (2021). "Deep learning–based text classification: a comprehensive review." *ACM Computing Surveys (CSUR)* 54 (3), 1–40.
- [7] Albahar, M. (2023). "A survey on deep learning and its impact on agriculture: challenges and opportunities." *Agriculture* 13 (3), 540.
- [8] Zhang, Y., Wang, S., Ji, G., and Phillips, P. (2014). "Fruit classification using computer vision and feedforward neural network." *Journal of Food Engineering* 143, 167–177.
- [9] Koç, D. G., and Vatandaş, M. (2021). "Classification of some fruits using image processing and machine learning." *Turkish Journal of Agriculture-Food Science and Technology* 9 (12), 2189–2196.
- [10] Valdez, P. (2020). "Apple defect detection using deep learning based object detection for better post harvest handling." arXiv preprint arXiv:2005.06089.
- [11] Hwa, L. S., and Te Chuan, L. (2024). "A brief review of artificial intelligence robotic in food industry." *Procedia Computer Science* 232, 1694–1700.
- [12] Pathmanaban, P., Gnanavel, B. K., Anandan, S. S., and Sathiyamurthy, S. (2023). "Advancing postharvest fruit handling through AI-based thermal imaging: applications, challenges, and future trends." *Discover Food* 3 (1), 27.
- [13] Li, X., Li, R., Wang, M., Liu, Y., Zhang, B., and Zhou, J. (2017). "Hyperspectral imaging and their applications in the non-destructive quality assessment of fruits and vegetables." In *Hyperspectral Imaging in Agriculture, Food and Environment*. IntechOpen.
- [14] Toivonen, P. M., and Brummell, D. A. (2008). "Biochemical bases of appearance and texture changes in fresh-cut fruit and vegetables." *Postharvest Biology and Technology* 48 (1), 1–14.
- [15] Whitelock, D. P., Bruswitz, G. H., and Stone, M. L. (2006). "Apple shape and rolling orientation." *Applied Engineering in Agriculture* 22 (1), 87–94.
- [16] Zhu, C., Ni, R., Xu, Z., Kong, K., Huang, W. R., and Goldstein, T. (2021). "Gradinit: Learning to initialize neural networks for stable and efficient training." *Advances in Neural Information Processing Systems* 34, 16410–16422.
- [17] Zhang, B., Huang, W., Gong, L., Li, J., Zhao, C., Liu, C., and Huang, D. (2015). "Computer vision detection of defective apples using automatic lightness correction and weighted RVM classifier." *Journal of Food Engineering* 146, 143–151.
- [18] Afzal, S. S., Kludze, A., Karmakar, S., Chandra, R., and Ghasempour, Y. (2023, October). "AgriTera: Accurate non-invasive fruit ripeness sensing via sub-terahertz wireless signals." In *Proceedings of the 29th Annual International Conference on Mobile Computing and Networking*, pp. 1–15.
- [19] Mamat, N., Othman, M. F., Abdoulghafor, R., Belhaouari, S. B., Mamat, N., and Mohd Hussein, S. F. (2022). "Advanced technology in agriculture industry by implementing image annotation technique and deep learning approach: A review." *Agriculture* 12 (7), 1033.
- [20] Abd El-aziz, A. A., Darwish, A., Oliva, D., and Hassanien, A. E. (2020). "Machine learning for apple fruit diseases classification system." In *Proceedings of the International Conference on Artificial Intelligence and Computer Vision (AICV2020)*, pp. 16–25. Springer International Publishing.

- [21] Ullah, W., Javed, K., Khan, M. A., Alghayadh, F. Y., Bhatt, M. W., Al Naimi, I. S., and Ofori, I. (2024). "Efficient identification and classification of apple leaf diseases using lightweight vision transformer (ViT)." *Discover Sustainability* 5 (1), 116.
- [22] Ismail, A. R., Azhary, M. Z. R., and Hitam, N. A. (2024, November). "Evaluating Adan vs. Adam: An Analysis of Optimizer Performance in Deep Learning." In *International Symposium on Intelligent Computing Systems*, pp. 251–263. Cham: Springer Nature Switzerland.
- [23] Boukili, M., and Jebbor, N. (2024, May). "Performance Optimization of Convolutional Neural Networks (CNN) in Multilabel Fruit Classification." In *2024 4th International Conference on Innovative Research in Applied Science, Engineering and Technology (IRASET)*, pp. 1–6. IEEE.
- [24] Kujur, L., Gupta, V., and Singhal, A. (2025). "A hybrid multi-optimizer approach using CNN and GB for accurate prediction of citrus fruit diseases." *Discover Applied Sciences* 7 (3), 151.
- [25] Risdin, F., Mondal, P. K., and Hassan, K. M. (2020). "Convolutional neural networks (CNN) for detecting fruit information using machine learning techniques." *IOSR Journal of Computer Engineering* 22 (2), 1–13.